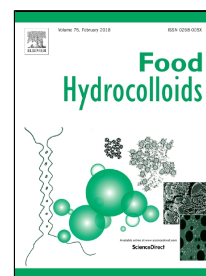


# Accepted Manuscript

Edible blend films of pectin and poly(ethylene glycol): Preparation and physico-chemical evaluation

Sanja Šešlija, Aleksandra Nešić, Jovana Ružić, Melina Kalagasidis Krušić, Sava Veličković, Roberto Avolio, Gabriella Santagata, Mario Malinconico



PII: S0268-005X(17)30449-6  
DOI: 10.1016/j.foodhyd.2017.10.027  
Reference: FOOHYD 4114  
To appear in: *Food Hydrocolloids*  
Received Date: 18 March 2017  
Revised Date: 10 October 2017  
Accepted Date: 21 October 2017

Please cite this article as: Sanja Šešlija, Aleksandra Nešić, Jovana Ružić, Melina Kalagasidis Krušić, Sava Veličković, Roberto Avolio, Gabriella Santagata, Mario Malinconico, Edible blend films of pectin and poly(ethylene glycol): Preparation and physico-chemical evaluation, *Food Hydrocolloids* (2017), doi: 10.1016/j.foodhyd.2017.10.027

This is a PDF file of an unedited manuscript that has been accepted for publication. As a service to our customers we are providing this early version of the manuscript. The manuscript will undergo copyediting, typesetting, and review of the resulting proof before it is published in its final form. Please note that during the production process errors may be discovered which could affect the content, and all legal disclaimers that apply to the journal pertain.

## Highlights

- Edible films from pectin and PEG were prepared.
- Film formation was supported by hydrogen bonding between components.
- Thermal and mechanical properties were affected by concentration and molecular weight of PEG.
- The increasing PEG concentration caused an increase in water vapor permeability.
- Films showed potential to be used in food packaging industry.

1 **Edible blend films of pectin and poly(ethylene glycol): Preparation and physico-chemical**  
2 **evaluation**

3  
4  
5 Sanja Šešlija<sup>1</sup>, Aleksandra Nešić<sup>2</sup>, Jovana Ružić<sup>2</sup>, Melina Kalagasidis Krušić<sup>\*3</sup>, Sava  
6 Veličković<sup>3†</sup>, Roberto Avolio<sup>4</sup>, Gabriella Santagata<sup>4</sup>, Mario Malinconico<sup>4</sup>

7  
8 <sup>1</sup>University of Belgrade, Institute of Chemistry, Technology and Metallurgy, Njegoševa 12, 11  
9 000 Belgrade, Serbia

10 <sup>2</sup>University of Belgrade, Vinča Institute for Nuclear Sciences, PO Box 522 11 001 Belgrade,  
11 Serbia

12 <sup>3</sup>University of Belgrade, Faculty of Technology and Metallurgy, Karnegijeva 4, 11 120 Belgrade,  
13 Serbia

14 <sup>4</sup>Institute for Polymers, Composites and Biomaterials, National Research Council of Italy, via  
15 Campi Flegrei 34, 80078 Pozzuoli (NA), Italy

16  
17 **Abstract**

18 The aim of this study was the development of novel polysaccharide based films intended to be  
19 used as edible food packaging material. The films were prepared by solution casting method  
20 using highly methoxylated pectin (PEC) and poly(ethylene glycol) (PEG) of various molecular  
21 weights (400, 600 and 1000 gmol<sup>-1</sup>) in different ratios (5:1, 3:1 and 1:1). The film formation was  
22 supported by hydrogen bonding between PEC and PEG, which was evidenced by means of ATR-  
23 FTIR and NMR analysis. TGA revealed that generally PEG behaves like a pro-degrading agent  
24 for pectin, except in the case of PEC/PEG film with a ratio of 1:1. Furthermore, DSC  
25 thermograms indicated that PEG1000 exists as a separate phase in the pectin matrix while the  
26 formulations with PEG400 and PEG600 showed mainly amorphous morphology. The addition of  
27 PEG enhanced the plasticization of PEC films, as evidenced by progressive decreasing of the  
28 glass transition temperature values ( $T_g$ ). The tensile test measurements showed that increasing  
29 concentration of PEG produced weaker and more flexible films. Due to the increased molecular  
30 mobility, the pectin phase became more permeable to water vapor as the PEG concentration  
31 increased. The obtained results showed that the combination of both polymers resulted in  
32 interesting bio-inspired edible films with the potential to compete with commercially used  
33 synthetic package materials.

34 **Keywords:** Pectin; Poly(ethylene glycol); Plasticization; Edible films; Hydrogen bonding

35  
36 **\*Corresponding author address:** University of Belgrade, Faculty of Technology and Metallurgy,  
37 Karnegijeva 4, 11 120 Belgrade, Serbia; Phone: +381 11 3303 730 fax: +381 11 3370 387  
38 *E-mail address:* [meli@tmf.bg.ac.rs](mailto:meli@tmf.bg.ac.rs)

39 <sup>†</sup> Deceased

## 41 1. Introduction

42 The food package must be designed to fulfill a number of important functions including  
43 containment and protection of food, maintaining food sensory quality and safety, extending shelf-  
44 life and retaining the beneficial effects of food products (Nanou et al, 2014). The use of synthetic  
45 materials is ubiquitous in food industry wherein they provide mechanical, chemical and microbial  
46 protection from the environment and allow product display. Petrochemical plastics, such as low-  
47 and high-density poly(ethylenes) (LDPE and HDPE), poly(propylene) (PP), poly(styrene) (PS)  
48 poly(ethylene terephthalate) (PET) and poly(amide) (PA) are well known as they play an  
49 important role in our daily lives (Marsh & Bugusu, 2007). Nevertheless, these plastic materials  
50 are responsible of the environmental problems related to their waste management, due to the huge  
51 volumes of plastic waste materials produced. Indeed, they do not readily degrade either in landfill  
52 or in composting facilities due to their biologically inert nature. In order to work towards a  
53 sustainable development, research is increasingly focusing its attention on eco-friendly packaging  
54 materials based on biodegradable polymers coming from renewable and available sources, as  
55 appealing eco-sustainable and cost-competitive bioplastics (Lambert, Sinclair & Boxall, 2014).  
56 Depending on their origin, biodegradable polymers can be synthetic or natural. Poly(vinyl  
57 alcohol) and polyesters are the most interesting among the former (Guimarães et al, 2015),  
58 whereas polysaccharides, proteins and polyesters produced by microorganisms, such as  
59 poly(lactic acid) (PLA) (Mahmood et al, 2016), poly(hydroxyalkanoates) (PHA), all of them  
60 referred to as biopolymers, belong to the latter (Angelini et al, 2014, Ortega-Toro et al, 2016).  
61 Polysaccharides such as cellulose, pectin, starch, chitosan, alginate, (Fabra et al, 2014, Cavallaro  
62 et al, 2011, Biddeci et al, 2016) are arousing huge scientific interest as renewable and available  
63 biopolymers potentially exploitable as novel eco-friendly food packaging material (Razzaq et al,  
64 2016).

65 Among them, pectin is one of the most abundant polysaccharide extracted from cell walls of most  
66 plants and fruits, such as apple, orange, lemon, and mango. It is an anionic polysaccharide  
67 formed by linear chain of poly- $\alpha$ -(1-4)-D-galacturonic acid with varying degrees of methyl  
68 esterification (Khotimchenko et al, 2008). The esterification degree (DE) determines the  
69 solubility of pectin, its gelling and film forming properties and therefore its industrial  
70 applicability. Actually, due to the simple and cytocompatible gelling mechanism, pectin has been  
71 exploited for different biomedical applications including drug delivery, gene delivery, wound  
72 healing and tissue engineering (Munarin, Tanzi & Petrini, 2012). As a matter of fact, the gelling  
73 properties of this polysaccharide can be specifically tuned, playing a key role in several  
74 applications. As an example, due to its ability to form a gel in acidic conditions, pectin has been  
75 widely used in food and beverage industries, as a thickening and gelling agent and as colloidal  
76 stabilizer in food products such as jams, yogurt drinks, fruity milk drinks, and ice cream (Laurent  
77 & Boulenguer, 2003). Being biodegradable, biocompatible and edible biopolymer, pectin  
78 represents a suitable polymer for the development of bio-based films for food packaging. Despite  
79 these advantages, pectin films are far from being appealing from the application point of view,  
80 because of their poor chemo-physical properties and unsuitable mechanical performances.

81 Furthermore, there are numerous drawbacks related to the film-forming process by means of  
82 casting method. Like most of the polysaccharides, pectin is glassy at room temperature, so its  
83 shrinkage following the evaporation of water or rapid drying, causes defects such as cracks or  
84 curling in the films (Obara & McGinity, 1995). These films are often brittle and stiff due to  
85 extensive interactions between polymer molecules, so the addition of the corresponding  
86 plasticizers is required (Gennadios, Hanna & Kurth, 1997). Plasticizers decrease intermolecular  
87 forces between polymer chains, increasing their flexibility and extendibility. They act by  
88 interposing between macromolecular polymeric chains, reducing cohesion within the film and  
89 enhancing the free volume inside the film structure (Banker, 1966; Wojciechowska, 2012; Avolio  
90 et al, 2015). With respect to the specific system, the selection of a plasticizer is based on the  
91 compatibility and permanence of the plasticizer, the amount necessary for plasticization, and the  
92 desired physical properties of the films. The food-grade plasticizers most commonly used in  
93 blend with pectin, are poly(ethylene glycol) (PEG), glycerol, propylene glycol, and sorbitol  
94 (Aydinli & Tutas, 2000). Poly(ethylene glycol) is commercially available over a wide range of  
95 molecular weights from 300  $\text{gmol}^{-1}$  to 10000  $\text{gmol}^{-1}$ , and due to excellent biocompatibility and  
96 non-toxicity, it is often blended or compounded with other polymers (Zhang et al, 2002). With  
97 reference to the other reported polysaccharide based films, it was shown that PEG of lower  
98 molecular weights exhibits better plasticizing effect. The increasing molecular weight of PEG  
99 caused the decrease in its polarity and solubility, as well as in its ability to interact with polymer  
100 chains (Turhan, Sahbaz & Guner, 2001). Also, the PEGs of higher molecular weights are solids,  
101 so they might crystallize and cause phase separation.  
102 In this study, we evaluated the plasticizing effect of poly(ethylene glycol) on the properties of  
103 pectin based films. The films were prepared by blending apple pectin (PEC) and poly(ethylene  
104 glycol) (PEG) of various molecular weights (400, 600 and 1000  $\text{gmol}^{-1}$ ) in different ratios (5:1,  
105 3:1 and 1:1). The investigation of structural (FTIR, NMR), bulk (DSC, TGA) and macroscopic  
106 properties (tensile tests and WVP) of PEC/PEG films have been discussed in order to set up new,  
107 eco-sustainable materials for edible food packaging application.

108

109

## 110 **2. Materials and methods**

### 111 **2.1 Raw materials**

112 Pectin from apples with a 70–75% esterification degree, DE, was purchased from the Sigma-  
113 Aldrich Company (USA). Poly(ethylene glycol) of different molecular weights (400, 600 and  
114 1000  $\text{gmol}^{-1}$ ) were all supplied by Merck (Germany).

### 115 **2.2 Film preparation**

116 Neat and plasticized films were obtained from aqueous solutions containing 2% w/v of pectin at  
117 50 °C in the presence of few drops of 0.1 M HCl (solutions were adjusted to pH 3). The  
118 previously calculated amount of PEG (with specified molecular weight of 400, 600 and 1000  
119  $\text{gmol}^{-1}$ ) was added to the single pectin solution in order to obtain mixtures with different

120 PEC/PEG weight ratios (5:1, 3:1 and 1:1), as shown in Table 1. The PEC/PEG solutions were  
 121 cast into circular shape Teflon molds (11 cm in diameter) and dried in an oven at 50 °C for 48 h.

### 122 2.3 ATR-FTIR analysis

123 Attenuated Total Reflection Fourier Transform Infrared (ATR-FTIR) spectroscopy was carried  
 124 out on the surface of PEC/PEG films using a Perkin Elmer Spectrum 100 spectrometer, equipped  
 125 with a Universal ATR diamond crystal sampling accessory. All the samples were analysed at 25  
 126 °C. Spectra were collected as an average of 16 scans in the range 4000–480 cm<sup>-1</sup>, with a  
 127 resolution of 4 cm<sup>-1</sup>. Prior to measurements, the samples were kept for 24 h at 60 °C under  
 128 vacuum.

### 129 2.4 NMR analysis

130 Nuclear magnetic resonance (<sup>13</sup>C NMR) spectroscopy was used for addressing the chemical  
 131 composition and structure of PEC/PEG films. Cross-polarization (CP) carbon spectra were  
 132 recorded on a Bruker Avance II 400 spectrometer operating at a static field of 9.4 T, equipped  
 133 with a 4 mm MAS probe and using a <sup>1</sup>H  $\pi/2$  pulse width of 3.0  $\mu$ s, a contact time of 2 ms and a  
 134 repetition time of 4 s. Finely cut samples were packed into 4 mm zirconia rotors sealed with Kel-  
 135 F caps and spun at a spinning speed of 10 kHz.

136  
 137 Table 1. Composition of the PEC/PEG films

Sample	Blending ratio	Sample ID*
PEC/PEG 400	5:1	P5/400
	3:1	P3/400
	1:1	P1/400
PEC/PEG 600	5:1	P5/600
	3:1	P3/600
	1:1	P1/600
PEC/PEG 1000	5:1	P5/1000
	3:1	P3/1000
	1:1	P1/1000

138 *\*The samples are designated to point out the PEC/PEG ratio (5, 3, and 1) as well as the molecular weight*  
 139 *of PEG used in the specific formulation (400, 600, and 1000 g mol<sup>-1</sup>).*

140  
 141 2.5 Mechanical analysis  
 142 Mechanical properties were performed using Instron dynamometer model 1185, equipped with a  
 143 1 kN load cell, according to the ASTM D638 (2010) standard test method at 23 ± 2 °C and 45 ±  
 144 5% relative humidity (RH). Dumbbell-shaped films (4 mm wide, 26.73 mm long and 0.05 mm  
 145 thick) were used and tested at a crosshead speed of 2 mm min<sup>-1</sup>. Prior to measurements, all the  
 146 films were conditioned at 25 °C and 50% RH for 48 h.

147

148

## 149 2.6 Thermal analysis

150 Differential Scanning Calorimetry (DSC) was performed using a TA DSC-Q2000 instrument  
151 equipped with a TA Instruments DSC cooling system under a nitrogen purge gas flow of 30 mL  
152  $\text{min}^{-1}$ . Indium was used to calibrate the calorimeter. Approximately 6 mg of the samples were  
153 sealed in aluminum pans and analyzed. In order to estimate the influence of the residual water on  
154 the thermal properties of the pectin films, two different DSC measurements were performed. In  
155 the first one, all the samples were placed in hermetic aluminum pans, in order to preserve their  
156 water content. The heating run ranged from -80 to +100 °C, with heating rate of 20 °C  $\text{min}^{-1}$ .

157 In the second test, all the specimens were equilibrated at -80 °C and heated up to 100 °C at 20  
158 °C/min. Then an isotherm step was performed at 100 °C for 30 min in order to remove the free  
159 and bound water. Afterwards, the samples were cooled up to -80 °C at 10 °C/min, thermally  
160 stabilized for 1 min at then re-heated up to 200 °C at 20 °C/min. For each sample, data analysis  
161 was averaged on a set of three measurements.

162 Thermogravimetric analysis (TGA) was performed by means of a Mettler-Toledo TG-SDTA 851,  
163 under nominal nitrogen flow of 30 mL $\text{min}^{-1}$ , in the temperature range from 25 to 800 °C and at  
164 the heating rate of 20 °C  $\text{min}^{-1}$ . The measurements were performed on samples of about 5 mg,  
165 placed in ceramic crucibles and for each sample, thermogravimetric tests were performed in  
166 triplicate. The obtained values of thermogravimetric and DSC parameters were repeatable  
167 within  $\pm 3\%$ .

## 168 2.7 Scanning electron microscopy

169 Morphological analysis of the film surfaces was performed using a Jeol JSM 5800 Scanning  
170 Electron Microscope with an acceleration voltage of 20 kV. The surfaces of the PEC/PEG films  
171 were coated with platinum under vacuum using a Polaron CS502 sputter coater before the  
172 analysis.  
173

## 174 2.8 Water vapor permeability (WVP)

175 WVP tests were conducted according to ASTM E96 standard method. The samples with exposed  
176 area of 6.54  $\text{cm}^2$  were sealed over a circular opening of permeation cells (BYK-Gardner) filled  
177 with distilled water. These cells were kept in oven at 25 °C under 50% RH. After the system  
178 reached steady state conditions, the weight change of the cell was measured every 2 h. Each film  
179 was tested three times to confirm repeatability of measurements. The standard deviation was  
180  $\pm 10\%$ .

181 The weight losses of films were plotted with respect to time, and the linear least-square method  
182 was used for the calculation of the parameters given by Equation 1 (Gennadios, Hanna & Kurth,  
183 1997):

$$184 \quad WVP = \frac{L \cdot WVTR}{A \cdot \Delta p} \quad (1)$$

186

187 where WVTR is the water vapor transmission rate of films ( $\text{g s}^{-1}$ ),  $L$  is average thickness of the  
188 film (mm),  $A$  is the permeation area ( $\text{mm}^2$ ),  $\Delta p$  is the difference in water vapor pressure between  
189 the two exposed sides of the film (Pa).

190  
191

### 192 3. Results and discussion

193 The film preparation showed to be successful for all the investigated PEC/PEG ratios. The  
194 solution casting method applied hereby has proven to be an effective procedure to obtain visually  
195 uniform films with homogeneous and smooth surfaces without pores or cracks. The light-yellow  
196 coloration, originated from the pectin component, could be observed for all of the investigated  
197 samples (Fig.1).

198

199 Fig.1. Visual appearance of the P3/400 film.

#### 200 3.1 ATR-FTIR spectroscopy

201 Infrared Spectroscopy represents a valid tool to assess the physical or chemical interactions  
202 between components in polymeric blend systems. ATR-FTIR spectra related to P1/400 and  
203 P5/400, P1/600 and P5/600, and P1/1000 and P5/1000 films and neat pectin in the range from  
204 2000 to  $800\text{ cm}^{-1}$  are shown in Figure 2.

205

206 Fig.2. ATR-FTIR spectra of a) P1/400 and P5/400, b) P1/600 and P5/600, c) P1/1000 and  
207 P5/1000 films.

208

209 In particular, the strong absorption bands occurring at  $1737$  and  $1605\text{ cm}^{-1}$  are attributed to the  
210 ester carbonyl ( $-\text{COOCH}_3$ ) groups and asymmetrical stretching vibration of carboxylate ion  
211 ( $\text{COO}^-$ ). The intensity of  $-\text{COOCH}_3$  band is higher if compared to the one of carboxylated group,  
212 which is characteristic of a highly methoxylated pectin (Gnanasambandan & Proctor, 2000).

213 The so called “fingerprint” peaks observed at  $1145$ ,  $1097$  and  $1012\text{ cm}^{-1}$  were assigned to the  
214 symmetric stretching vibrations of C-O-C, C-OH and C-C bonds from the ring structure of the  
215 pectin (Assifaoui et al, 2010).

216 After the addition of PEG 400, the peaks assigned to the ester and carboxylate stretching  
217 vibrations of neat pectin were shifted to higher frequencies (Table 2). In the case of the  
218 carboxylate band, the shifts were more pronounced for the samples with lower content of PEG.

219 The addition of PEG1000 caused prominent shifts of the peak attributed to the stretching  
220 vibration of carboxylate group, but only a slight shift of the peak deriving from the stretching of  
221 C=O group (Table 2).

222

223

224

225

226



227 Table 2. The vibrational modes of carbonyl region

Samples/Band frequency (cm <sup>-1</sup> )	COO <sup>-</sup> (asym)	COOCH <sub>3</sub>
Neat pectin	1605	1737
P1/400	1630	1747
P5/400	1615	1743
P1/600	1627	1745
P5/600	1610	1740
P1/1000	1639	1736
P5/1000	1628	1739

228  
 229 The appearance of new peaks associated with possible chemical interactions between pectin and  
 230 PEG were not evidenced. All the shifts observed in the corresponding PEC/PEG spectra may be  
 231 attributed to the interactions between pectin and PEG via formation of hydrogen bonds (Wang,  
 232 Waterhouse & Sun-Waterhouse, 2013).

### 233 234 3.2 NMR analysis

235 The <sup>13</sup>C NMR spectroscopy was used to gather more information about interactions between  
 236 pectin and PEG. There were no significant differences between spectra of PEC/PEG films with  
 237 various film compositions except for the relative intensity of pectin and PEG signals, hence, only  
 238 spectra of the neat pectin, P1/400, P1/1000 and PEG 1000 are shown in Figure 3a.

239 The main signals of pectin repeating unit (D-galacturonic acid) are observed at ≈ 100 ppm (C-1),  
 240 170 ppm (C-6, carboxyl) and overlapped in the region 70 – 90 ppm (C-2 and C-3 at 70 ppm, C-5  
 241 at ≈ 72 ppm, C-4 at ≈ 80 ppm). A strong CH<sub>3</sub>O signal is observed at 53 ppm, due to the high  
 242 degree of esterification of the pectin under investigation. No change in the ratio between the area  
 243 of methoxy peak and the other pectin signals was found, showing that the degree of esterification  
 244 did not change during the preparation of the materials.

245 The spectra of the films containing PEG differed only slightly from that of the neat pectin. The  
 246 signals of the PEG were clearly observed at 70.6 ppm (main chain CH<sub>2</sub>-O) and at 61.3 and 72  
 247 ppm (terminal CH<sub>2</sub>-O and CH<sub>2</sub>-OH) (Synytsya, Copíková & Brus, 2003). Carbon signals in PEG  
 248 were noticeably narrower than in pectin, pointing out a fast segmental motion. Also a slight  
 249 change in the shape of the complex C-1 and C-4 peak was observed, underlining an effect of PEG  
 250 on chain conformation of pectin. Interesting differences can be evidenced in the shape of the  
 251 peaks in the carboxyl region of PEG containing materials. The downfield shoulder present in  
 252 pectin spectrum, assigned to free carboxyl/carboxylate groups (Zhu et al, 2014), is not observed  
 253 in P1/400 and P1/1000 samples, while the main peak is slightly shifted upfield (see inset of  
 254 Figure 3). This finding suggests a protonation of COO<sup>-</sup> groups of pristine pectin following the  
 255 treatment in acidic solutions and a possible involvement of these groups in hydrogen bonding  
 256 with PEG. A significant conversion of the carboxylic groups of pectin to esters by reaction with  
 257 PEG can be ruled out, as in this case a new signal for the esterified CH<sub>2</sub>O- of PEG should be  
 258 present in the range 62 – 65 ppm.

259 Fig.3. a)  $^{13}\text{C}$  NMR spectra of the neat pectin and the PEC/PEG film. The carboxyl region is  
 260 highlighted in the figure inset. Spinning sidebands are marked by a dot. b) Hydrogen bonding  
 261 between PEG and PEC chains.

262 According to the FTIR and NMR analyses, the PEC/PEG film formation was supported by  
 263 hydrogen bonding between PEC and PEG and could be established between carboxyl,  
 264 methylester and hydroxyl groups of pectin and oxygen atoms of the PEG. However, the  
 265 methylester substitution pose more steric hindrance, so the interactions between methylester  
 266 groups and oxygen atom from PEG could be considered as negligible (Embuscado, 2014).  
 267 Therefore, the most probable interactions are between COOH groups from the pectin and ether-  
 268 hydroxyl groups of PEG (Fig.3b). The pKa value for the pectin with DE of 72.9% has been found  
 269 to be 3.5 (Michel, Thibault & Doublier, 1984). So, in order to avoid the ionization of  $-\text{COOH}$   
 270 groups and electrostatic repulsion within the pectin chains, all the samples were synthesized  
 271 under the pH value of 3 as above mentioned in the experimental section.

### 272 3.3 Mechanical analysis

273 Mechanical parameters such as tensile strength (TS) and Young's modulus of elasticity (E) are  
 274 reliable indicators for the cracks formation in polymeric films used for packaging (Robertson,  
 275 2009). Table 3 summarizes the values of TS and E modulus for the PEC/PEG films, as well as  
 276 the values of TS and E parameter for commercial synthetic package materials adopted from  
 277 literature. The thickness of the PEC/PEG films was approximately 50  $\mu\text{m}$ . The neat pectin film  
 278 was very fragile and it was impossible to determine its tensile strength and E modulus.

279 Table 3. Tensile strength (TS) and Young's modulus of elasticity (E) for the PEC/PEG films

Sample	TS, MPa	E, GPa	Reference
P5/400	31 $\pm$ 5	0.29 $\pm$ 0.04	
P3/400	21 $\pm$ 3	0.17 $\pm$ 0.02	
P1/400	13 $\pm$ 2	0.10 $\pm$ 0.01	
P5/600	36 $\pm$ 5	0.39 $\pm$ 0.06	
P3/600	29 $\pm$ 4	0.34 $\pm$ 0.05	
P1/600	20 $\pm$ 3	0.22 $\pm$ 0.03	This work
P5/1000	48 $\pm$ 7	0.45 $\pm$ 0.07	
P3/1000	28 $\pm$ 4	0.31 $\pm$ 0.05	
P1/1000	12 $\pm$ 2	0.07 $\pm$ 0.01	
LDPE	7-17	0.14-0.30	
HDPE	20-40	0.7-1.4	Mark,
PP	30-40	1-2	2007
PS	30-60	2.4-3.2	

280  
 281 As expected, the mechanical properties of the films changed considerably with the use of PEG  
 282 plasticizers. The mechanical property parameters provided by the tensile test measurements are

283 shown in Table 3. Increasing concentration of PEG produced weaker (TS decreased) and more  
284 flexible films (E modulus decreased). These results can be explained as a consequence of the  
285 reduced intermolecular forces between pectin chains after the PEG was added. With exception of  
286 P1/1000 film, the increase in molecular weight of PEG led to more rigid behavior (E increased)  
287 resulting from the denser chain packing within films (Pasini Cabello et al, 2015). The similar  
288 trend was observed for poly(lactide)/PEG blends reported by Li et al (2015). The lowest TS  
289 values obtained for the P1/1000 film indicated that the addition of PEG 1000 above 33 wt %  
290 probably caused the disruption of the PEC phase continuity and an extensive separation of PEG  
291 phase. Compared to the other pectin based films reported in literature, the tensile strength values  
292 obtained for the PEC/PEG films were significantly higher (12-48 MPa). This could be caused by  
293 the differences in the way of preparation, pectin type and final thickness of the films (Wang,  
294 Waterhouse & Sun-Waterhouse, 2013; Synytsya, Copíková & Brus, 2003; Zhu et al, 2014). For  
295 comparison, the relevant mechanical parameters of the commercially used synthetic package  
296 material are also presented in Table 3.

### 297 3.4 Thermal analysis

298 TGA and DSC analyses were performed to get insight on the properties of the PEC/PEG film at  
299 molecular level. Figure 4 shows the TGA and DTG curves of the neat pectin powder and the  
300 PEC/PEG films.

301 Fig.4. The TGA (a, b) and DTG (c, d) curves of neat pectin powder and PEC/PEG films.

302 The TGA/DTG curve of the neat pectin showed two weight loss steps. The first step, in the  
303 temperature range from 50 to 100 °C was assigned to the vaporization of water, and the second  
304 one, in the temperature range from 200 to 320 °C (reaching maximum at 240 °C), was attributed  
305 to the decomposition of the pectin chain (Fig.4) (Tripathi, Mehrotra & Dutta, 2010). Thermal  
306 degradation of pure PEG is a one-step process taking place in a temperature range from 310 to  
307 390 °C, depending on its molecular weight (Cavallaro, Lazzara & Milioto, 2013; Yanshan et al,  
308 2014). The degradation process of the PEC/PEG films exhibited three degradation stages: a)  
309 elimination of water from 50 to 100 °C; b) degradation of the pectin chains around 240 °C and c)  
310 decomposition of the PEG molecule from 300 to 400 °C. Based on the shape of weight loss  
311 curves (Fig.4 a,b) and DTG curves (Fig.4 c,d) it could be concluded that degradation of  
312 PEC/PEG films was affected by the concentration and molecular weight of PEG.

313 The onset temperatures were determined based on DTG curves (Table 4). As shown in Figure  
314 4 c, d the onset degradation temperatures of the PEC/PEG films were slightly anticipated  
315 compared to the neat pectin (225 °C) and this trend was more pronounced for higher PEG  
316 contents in the films. Contrary, sample P5/1000 delayed onset degradation temperature in  
317 comparison to the neat pectin.

318 The glass transition temperature was detected for all the samples, except for the P1/1000 film  
319 where the  $T_g$  was covered by wide endothermic peak related to the melting of the PEG1000  
320 (Fig.5, Table 5). The non isothermal DSC run showed the  $T_g$  value of neat pectin at 51 °C. Except  
321 for the P5/1000 and P3/1000, the  $T_g$  values of all considered PEC/PEG films were below the  $T_g$

322 value of neat pectin. In addition, the  $T_g$  values of the films were lower when the PEG content was  
 323 up to 33 wt% (P5 and P3) while for the further increase of the PEG in system  $T_g$  values shifted to  
 324 higher temperatures (P1).

325 As mentioned before, the addition of PEG produced micro-structural changes in the polymer  
 326 matrix by involving a reduction in the intermolecular forces between polymer chains, so it was  
 327 expected for  $T_g$  values to be decreased (Martucci, Accareddu & Ruseckaite, 2012). The strong  
 328 melting peak observed for all P/1000 films confirmed the formation of two phase systems. The  
 329 P3/400, P5/400, P3/600 and P5/600 thermograms did not show melting peaks, indicating a good  
 330 miscibility of the components and mainly amorphous morphology (Fig.5).

331

332 Table 4. The onset and degradation temperatures obtained by TGA

Sample	Onset, °C	Pectin degradation, °C	PEG degradation, °C
Neat pectin	225	240	-
P5/400	223	237	372
P3/400	222	237	321
P1/400	216	237	312
P5/600	223	238	370
P3/600	221	238	351
P1/600	216	238	366
P5/1000	228	243	382
P3/1000	223	241	388
P1/1000	220	238	388

333

334 The increasing PEG1000 concentration caused the shifting of enthalpy ( $\Delta H_m$ ) and melting point  
 335 ( $T_m$ ) values from 1.21 J/g and 28.65 °C (P5/1000) to 24.75 J/g and 30.91 °C (P1/1000),  
 336 respectively, indicating that blending of these components was affected by both concentration  
 337 and molecular weight of PEG. Hence, the highest  $T_g$  values of the PEC/PEG films were obtained  
 338 in presence of PEG1000, wherein the plasticizing effect was partly suppressed due to limited  
 339 miscibility of the components over the investigated concentration ranges.

340 Fig.5. DSC scans of non-dried PEC/PEG films of various compositions.

341 When the free unbound water was removed by first heating run and the  $T_g$  value was determined  
 342 during the second heating run (dried films), the  $T_g$  of the PEC/PEG films was significantly shifted  
 343 to higher values, confirming the strong influence of residual water on the chains mobility. The  $T_g$   
 344 of the neat pectin powder was found to be at 133 °C. An increase in PEG concentration caused  
 345 the decrease in  $T_g$  values due to enhanced chain mobility (See Table 5). During the cooling  
 346 process, crystallization peak of PEG could be seen for all the PEC/PEG films, while the melting  
 347 peak of PEG was observed in the second heating run. Nevertheless, with a decrease of PEG  
 348 concentration in pectin matrix, the enthalpy of melting (which correlates with crystallinity of

349 PEG in films) decreased from 19.65 J/g to 2.12 J/g (PEG400), 26.45 J/g to 1.47 J/g (PEG600)  
 350 and 29.70 J/g to 2.29 J/g (PEG1000), respectively. This dependence confirmed some miscibility  
 351 between pectin and PEG even if phase separation of PEG 1000 occurred. The melting  
 352 temperature also decreased with decreasing concentration of PEG in films, ranging between 4.4  
 353 °C and 3.9 °C (PEG400), 17.6 °C and 11.9 °C (PEG600) and 36.4 °C and 32.4 °C (PEG1000).  
 354 The trend related to the decrease in  $T_m$  values of PEG with an increasing pectin concentration  
 355 may be attributed to the crystal size reduction, more pronounced crystalline defects or changes of  
 356 PEG's crystals structure (Alfonso & Russell,1986).

357  
 358 Table 5.  $T_g$  values of the PEC/PEG films obtained by nonisothermal and isothermal DSC scan

Sample	$T_g$ , °C	
	Non-dried samples	Dried samples
Neat pectin	50	133
P5/400	44	98
P3/400	42	95
P1/400	50	93
P5/600	47	113
P3/600	44	109
P1/600	46	94
P5/1000	54	127
P3/1000	51	118
P1/1000	covered by wide endothermic peak	110

359  
 360 3.5 SEM analysis  
 361 The SEM micrographs of the neat pectin and the PEC/PEG films with component ratio 5:1 and  
 362 3:1 were homogeneous with a flat surface without cavities (images not presented). At the highest  
 363 PEG concentration (blending ratio 1:1), there were no significant differences regarding the  
 364 surface morphology of P/400 and P/600 samples (images not presented), while the addition of  
 365 PEG 1000 caused prominently rougher and denser structure (Fig.6.). The numerous  
 366 inhomogeneous domains located on the P1/1000 film surface could be the consequence of the  
 367 poor miscibility of the components over the given concentration range, followed by an extensive  
 368 separation of PEG 1000 phase.

369 Fig.6. SEM micrographs of the P1/400 (a, a1) and P1/1000 (b, b1) films at various  
 370 magnifications.

### 371 3.6 Water vapor permeability

372  
 373 Generally, the addition of a plasticizer modifies the properties of the film by reducing the  
 374 intermolecular interactions between the polymer chains, thus increasing the WVP of the film.

375  
 376

377 Table 6. The WVP parameters of the PEC/PEG films

378	Sample	WVP x10 <sup>12</sup> , gm <sup>-1</sup> s <sup>-1</sup> Pa <sup>-1</sup>	Reference
	P5/400	292	
	P3/400	271	
	P1/400	470	
	P5/600	293	
	P3/600	410	
	P1/600	485	This work
	P5/1000	302	
	P3/1000	298	
	P1/1000	473	
	LDPE	0.067-0.087	
	HDPE	0.017-0.038	
	PP	0.023-0.046	Sung et al, 2013
	PS	0.11-0.46	

379  
 380 Based on the data given by Table 6, an increase of PEG amount in the films formulations led to  
 381 an increase in water vapor permeability, mainly due to the increased molecular mobility of pectin  
 382 chains. Another proposed reason could be the clustering of plasticizer molecules at high  
 383 concentrations, resulting in a discontinuous structure in film matrix (Cerqueira et al, 2012). The  
 384 WVP values varied from 2.7x10<sup>-10</sup> to 4.85x10<sup>-10</sup> gm<sup>-1</sup>s<sup>-1</sup>Pa<sup>-1</sup> and no significant influence with  
 385 respect to the molecular weight of PEG was found. The obtained values of water vapor  
 386 permeability were higher by several orders of magnitude than those reported for the films made  
 387 from PS, LDPE and HDPE, as shown in Table 6.

### 388 389 **Conclusions**

390 Pectin/poly(ethylene glycol) films were prepared successfully by solution casting method using  
 391 highly methoxylated pectin (PEC) and poly(ethylene glycol) (PEG) of various molecular weights  
 392 (400, 600 and 1000 gmol<sup>-1</sup>) in different ratios (5:1, 3:1 and 1:1). The film formation was  
 393 supported by the formation of hydrogen bonds, most probably established between carboxyl  
 394 groups from pectin and oxygen atoms from PEG. The increasing PEG concentration produced  
 395 weaker and more flexible films, while increase in molecular weight of PEG contributed to the  
 396 films rigidity. It was found that thermal stability of the PEC/PEG films was affected by the  
 397 concentration and molar mass of PEG. In general, the onset degradation temperatures of the  
 398 PEC/PEG films were slightly reduced compared to the neat pectin (225 °C) and this trend was  
 399 more pronounced at higher PEG concentrations. The highest T<sub>g</sub> values of the PEC/PEG films  
 400 were obtained in presence of PEG1000 indicating the most suppressed plasticizing effect of PEG  
 401 1000, probably due to the limited miscibility of the components. The two phase morphology of  
 402 P/1000 samples was additionally confirmed by SEM analysis. The WVP was increased by the  
 403 increase in PEG concentration, while it was not affected by its molecular weight. Finally, the  
 404 presented study revealed satisfactory performances of the investigated system to be used for

405 edible food packaging application. Still, in order to keep the eco-friendly approach and potential  
406 to compete with commercially available food package materials, additional efforts should be  
407 directed toward a further improvement of PEC/PEG films.

408

409

#### 410 **Acknowledgement**

411 The authors acknowledge funding from the Ministry of Education, Science and  
412 Technological Development of the Republic of Serbia, Bilateral Project Serbia-Italy No. 451-03-  
413 01231/2015-09/5, 172062 and III43009.

414

415

#### 416 **References**

417 Alfonso, C. C., Russell, T. P. (1986). Kinetics of Crystallization in Semicrystalline/amorphous  
418 Polymer Mixtures, *Macromolecules* 19 (4), 1143-1152.

419 Angelini, S., Cerruti, P., Immirzi, B., Santagata, G., Scarinzi, G., Malinconico, M. (2014). From  
420 biowaste to bioresource: Effect of a lignocellulosic filler on the properties of poly(3-  
421 hydroxybutyrate). *International Journal of Biological Macromolecules* 71, 163-173.

422 Assifaoui, A., Loupiac, C., Chambin, O., Cayot, P. (2010). Structure of calcium and zinc  
423 pectinate films investigated by FTIR spectroscopy, *Carbohydrate Research* 345, 929-933.

424 Avolio, R., Castaldo, R., Gentile, G., Ambrogi, V., Fiori, S., Avella, M., Cocca, M., Errico M.E.  
425 (2015). Plasticization of poly(lactic acid) through blending with oligomers of lactic acid: Effect  
426 of the physical aging on properties, *European Polymer Journal*, 66, 533-542.

427 Aydinli M, Tutas M. (2000). Water sorption and water vapor permeability properties of  
428 polysaccharide (Locust Bean Gum) based edible films. *Lebensmittel-Wissenschaft und –*  
429 *Technologie*, 33(1), 63-7.

430 Banker, G. S. (1966). Film coating theory and practice, *Journal of Pharmaceutical Sciences*,  
431 55(1), 81-89.

432 Biddeci G., Cavallaro G., Di Blasi F., Lazzara G., Massaro M., Milioto S., Parisi F., Riela S.,  
433 Spinelli G. (2016). Halloysite nanotubes loaded with peppermint essential oil as filler for  
434 functional biopolymer film, *Carbohydrate Polymers*, 152, 548-557.

435 Cavallaro, G., Lazzara G., Milioto, S. (2013). Sustainable nanocomposites based on halloysite  
436 nanotubes and pectin/polyethylene glycol blend, *Polymer Degradation and Stability* 98,12, 2529-  
437 2536.

438 Cavallaro G., Lazzara G., Milioto S. (2011). Dispersions of Nanoclays of Different Shapes into  
439 Aqueous and Solid Biopolymeric Matrices. Extended Physicochemical Study, *Langmuir* 27 (3),  
440 1158-1167.

- 441 Cerqueira, M.A., Souza, B.W.S., Teixeira, J.A. & Vicente, A.A. (2012). Effect of glycerol and  
442 corn oil on physicochemical properties of polysaccharide films – a comparative study, *Food*  
443 *Hydrocolloids*, 27, 175-184.
- 444 Embuscado, ME. (2014). *Functionalizing Carbohydrates for Food Applications: Texturizing and*  
445 *Bioactive/Flavor Delivery Systems*, DEStech Publications, Inc.
- 446 Fabra, M.J., López-Rubio, A., Lagaron, J.M. (2014). Biopolymers for food packaging  
447 applications, *Smart Polymers and their Applications*, 15, 476-509.
- 448 Garcia, MA., Martino, MN., Zaritzki, NE. (2000). Barrier properties of edible starch-based films  
449 and coatings, *Journal of Food Science*, 65(6), 941-7.
- 450 Gennadios, A., Hanna, M. A., Kurth, L. B. (1997). Application of edible coatings on meats,  
451 poultry and seafoods: a review, *LWT-Food Science and Technology*, 30(4), 337-350.
- 452 Gnanasambandan, R., Proctor, A. (2000). Determination of pectin degree of esterification by  
453 diffuse reflectance Fourier transform infrared spectroscopy, *Food Chemistry*, 68, 327-332.
- 454 Guimarães, M., Botaro, V., Novacke, K., Teixeira, F., Tonoli, G. (2015). Starch/PVA-based  
455 nanocomposites reinforced with bamboo nanofibrils, *Industrial Crops and Products* 70,72-83.
- 456 GurgelAdeodato Vieira, M., Altenhofen da Silva, M., Oliveira dos Santos, L., Masumi Beppu, M.  
457 (2011). Natural-based plasticizers and biopolymer films: A review, *European Polymer Journal*  
458 47, 254-263.
- 459 Khotimchenko, M.Y., Kolenchenko, E.A., Khotimchenko Y.S. (2008). Zinc-binding activity of  
460 different pectin compounds in aqueous solutions, *Journal of Colloid and Interface Science*, 323,  
461 216-222.
- 462 Lambert, S., Sinclair, CJ., Boxall, A. (2014). Occurrence, degradation and effects of polymer-  
463 based materials in the environment, *Review of Environmental Contamination and Toxicology*,  
464 227, 1-53.
- 465 Laurent, M. A., Boulenger, P. (2003). Stabilization mechanism of acid dairy drinks (ADD)  
466 induced by pectin, *Food Hydrocolloids*, 17 (4), 445-454.
- 467 Li, F-J., Liang, J-Z., Zhang, S-D., Zhu, B. (2015). Tensile Properties of Polylactide/Poly(ethylene  
468 glycol) Blends, *Journal of Polymers and Environment* 23, 407-415.
- 469 Mahmood, K., Aqdas, Z., Mohammad, N., Shazia, Z., Mohammad, M. (2016). Recent  
470 developments and future prospects on bio-based polyesters derived from renewable resources: A  
471 review, *International journal of biological macromolecules* 82, 1028-1040.
- 472 Mark, JE. (2007). *Physical Properties of Polymers Handbook Second*, Springer  
473 Science&Business Media, LLC.



- 474 Marsh, K., Bugusu, B. (2007). Food packaging—roles, materials and environmental issues,  
475 *Journal of Food Science* 72(3), 39-55.
- 476 Martucci, J.F., Accareddu, A.E.M., Ruseckaite, R.A. (2012). Preparation and characterization of  
477 plasticized gelatin films cross-linked with low concentrations of Glutaraldehyde, *Journal of*  
478 *Material Science* 47, 3282-3292.
- 479 Michel, F., Thibault, J.F., Doublier, J.L.(1984). Viscosimetric and potentiometric study of high-  
480 methoxylpectins in the presence of sucrose, *Carbohydrate Polymers* 4, 298-297.
- 481 Munarin, F., Tanzi, M.C., Petrini P. (2012). Advances in biomedical applications of pectin gels.  
482 *International Journal of Biological Macromolecules*, 51, 681– 689.
- 483 Nanou, P., Ragaert, P., Vandemoortele, A., Verguldt, E., De Meulenaer, B., Devlieghere, F.  
484 (2014). Use of biobased materials for modified atmosphere packaging of short and medium shelf-  
485 life food products, *Innovative Food Science & Emerging Technologies* 26, 319-329.
- 486 Obara, S., McGinity, JW. (1995). Influence of processing variables on the properties of free films  
487 prepared from aqueous polymeric dispersions by a spray technique, *International Journal of*  
488 *Pharmaceutics* 37, 849-53.
- 489 Ortega-Toro, R., Santagata, G., Gomez d' Ayala, G., Cerruti, P., Oliag, PT., Amparo Chiralt Boix,  
490 M., Malinconico, M. (2016). Enhancement of interfacial adhesion between starch and grafted  
491 poly( $\epsilon$ -caprolactone), *Carbohydrate Polymers*, 147, 16-27.
- 492 Pasini Cabello S.D., Takara E.A., Marchese J., Ochoa N.A. (2015). Influence of plasticizers in  
493 pectin films: Microstructural changes, *Materials Chemistry and Physics* 162, 491-497.
- 494 Razzaq, HA.A., Pezzuto, M., Santagata, G., Silvestre, C., Cimmino, S., Larsen, N., Duraccio, D.  
495 (2016). Barley  $\beta$ -glucan-protein based bioplastic film with enhanced physicochemical properties  
496 for packaging. *Food Hydrocolloids* 58, 276-283.
- 497 Robertson, GL. (2009). *Food Packaging and Shelf Life: A Practical Guide*, CRC Press
- 498 Sung, S-Y., Sin, LT., Tee, T-T., Bee, S-T., Rahmat, AR., Rahman, WaWA., Tan, A-C.,  
499 Vikhraman, M. (2013). Antimicrobial agents for food packaging applications, *Trends in Food*  
500 *Science and Technology* 33, 110-123.
- 501 Synytsya A., Copíková J., Brus J. (2003).  $^{13}\text{C}$  CP/MAS NMR spectra of pectins: a peak-fitting  
502 analysis in the C-6 region. *Czech Journal of Food Science*, 21, 1-12.
- 503 Tripathi, S., Mehrotra, G.K., Dutta, P.K. (2010). Preparation and physicochemical evaluation of  
504 chitosan/poly(vinyl alcohol)/pectin ternary film for food-packaging applications, *Carbohydrate*  
505 *Polymers*, 79 (3) 711–716.
- 506
- 507 Turhan, K. N., Sahbaz, F., Guner, A. (2001). A spectrophotometric study of hydrogen bonding in  
508 methylcellulose-based edible films plasticized by polyethylene glycol. *Journal of Food Science*,  
509 66 (1) 59-62.

- 510 Wang, W., Waterhouse, G. I., Sun-Waterhouse, D. (2013). Co-extrusion encapsulation of canola  
511 oil with alginate: effect of quercetin addition to oil core and pectin addition to alginate shell on  
512 oil stability. *Food Research International*, 54(1), 837-851.
- 513 Wojciechowska P. (2012). The effect of concentration and type of plasticizer on the mechanical  
514 properties of cellulose acetate butyrate organic– inorganic hybrids. In: Luqman M., *Recent*  
515 *advances in plasticizers* (pp.141–64), In Tech publishing.
- 516 Yanshan, L., Shujun, W., Hongyan, L., Fanbin, M., Huanqing, M., Wangang, Z. (2014).  
517 Preparation and characterization of melamine/formaldehyde/ polyethylene glycol crosslinking  
518 copolymers as solid–solid phase change materials, *Solar Energy Materials & Solar Cells* 127, 92-  
519 97.
- 520 Zhang, M. L., Gong, X. H., Zhao, Y. D., Zhang, N. M. (2002). Properties and biocompatibility of  
521 chitosan films modified by blending with PEG, *Biomaterials*, 23(13), 2641-2648.
- 522 Zhu, X., Liu, B., Zheng, S., Gao, Y. (2014). Quantitative and structure analysis of pectin in  
523 tobacco by <sup>13</sup>C CP/MAS NMR spectroscopy. *Analytical Methods*, 6, 6407-6413.
- 524  
525  
526  
527  
528  
529  
530  
531  
532  
533  
534  
535  
536  
537  
538  
539  
540  
541  
542  
543  
544  
545  
546  
547  
548  
549  
550  
551  
552  
553  
554

555 Figure captions

- 556
- 557 Fig.1. Visual appearance of the P3/400 film.
- 558 Fig.2. ATR-FTIR spectra of a) P1/400 and P5/400, b) P1/600 and P5/600, c) P1/1000 and  
559 P5/1000 films.
- 560
- 561 Fig.3. a)  $^{13}\text{C}$  NMR spectra of the neat pectin and the PEC/PEG film. The carboxyl region is  
562 highlighted in the figure inset. Spinning sidebands are marked by a dot. b) Hydrogen bonding  
563 between PEG and PEC chains.
- 564 Fig.4. The TGA (a, b) and DTG (c, d) curves of neat pectin powder and PEC/PEG films.
- 565 Fig.5. DSC scans of non-dried PEC/PEG films of various compositions.
- 566 Fig.6. SEM micrographs of the P1/400 (a, a1) and P1/1000 (b, b1) films at various  
567 magnifications.

568

569

570

571

572

573

574

575

576

577

578

579

580

581

582

583

584

585

586

587

588

589

590

591

592

593

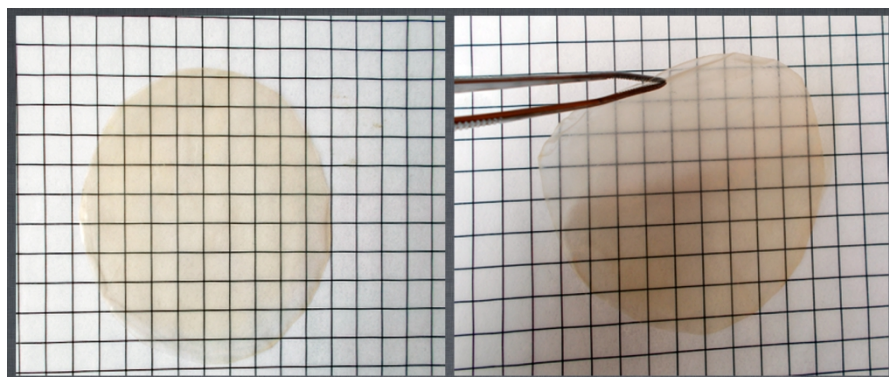
594

595

596

597 Figure 1

598



599  
600

601

602

603

604

605

606

607

608

609

610

611

612

613

614

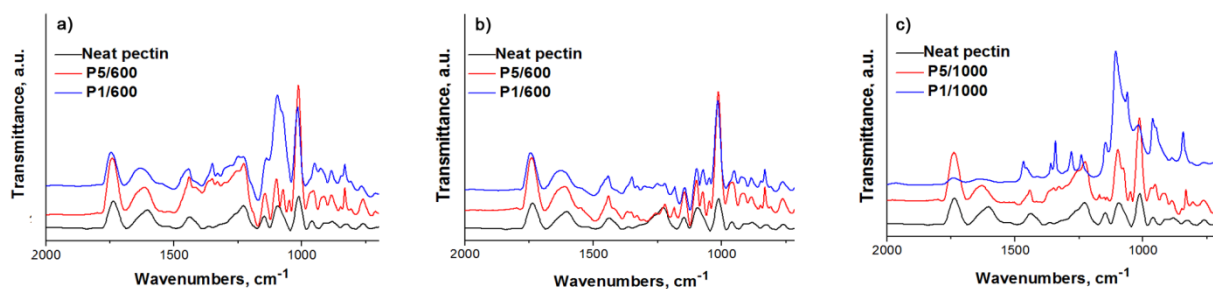
615

616

617

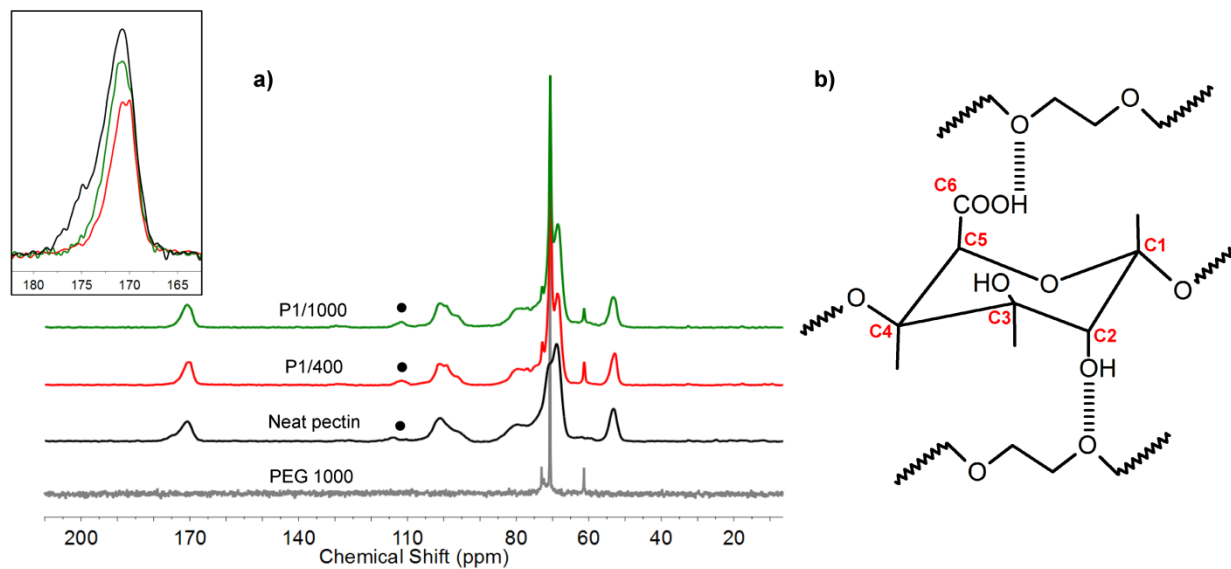
618

619 Figure 2

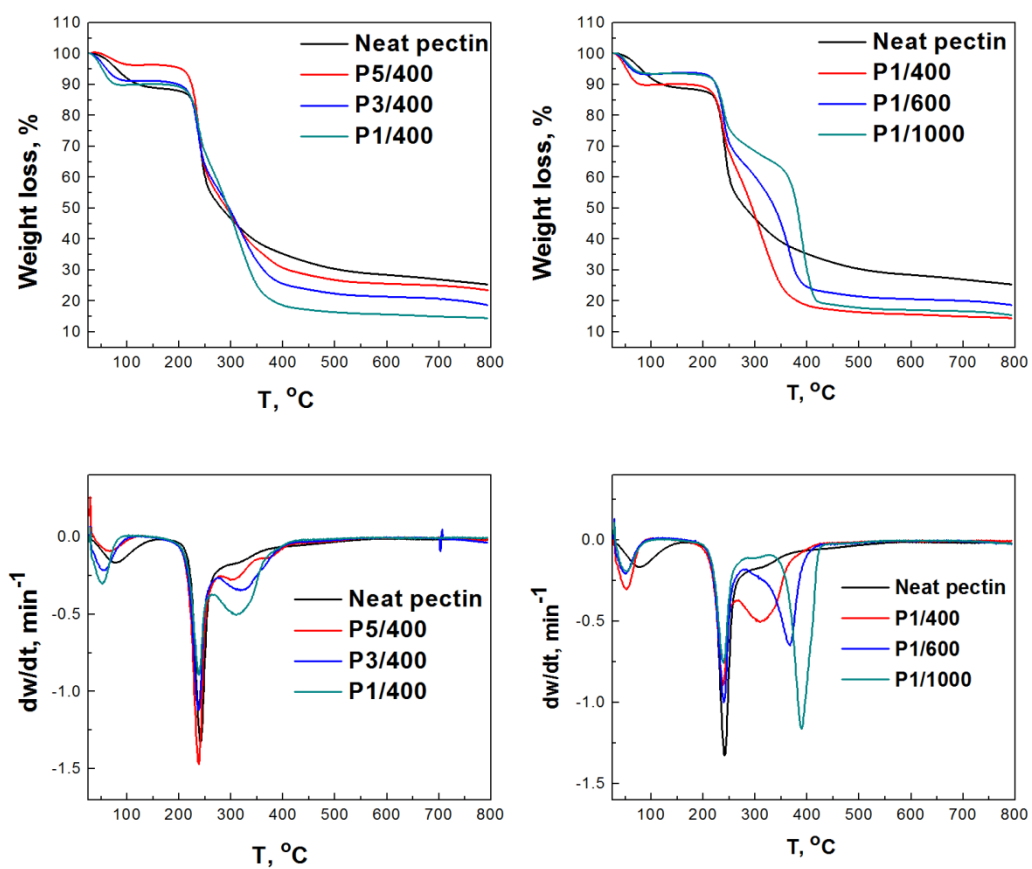
620  
621622  
623  
624  
625  
626  
627  
628  
629  
630  
631  
632  
633  
634  
635  
636  
637  
638  
639  
640  
641  
642  
643  
644  
645  
646  
647  
648  
649  
650  
651  
652  
653  
654  
655  
656  
657  
658  
659  
660

ACCEPTED MANUSCRIPT

661 Figure 3

662  
663664  
665  
666  
667  
668  
669  
670  
671  
672  
673  
674  
675  
676  
677  
678  
679  
680  
681  
682  
683  
684  
685  
686  
687  
688  
689  
690  
691  
692  
693  
694

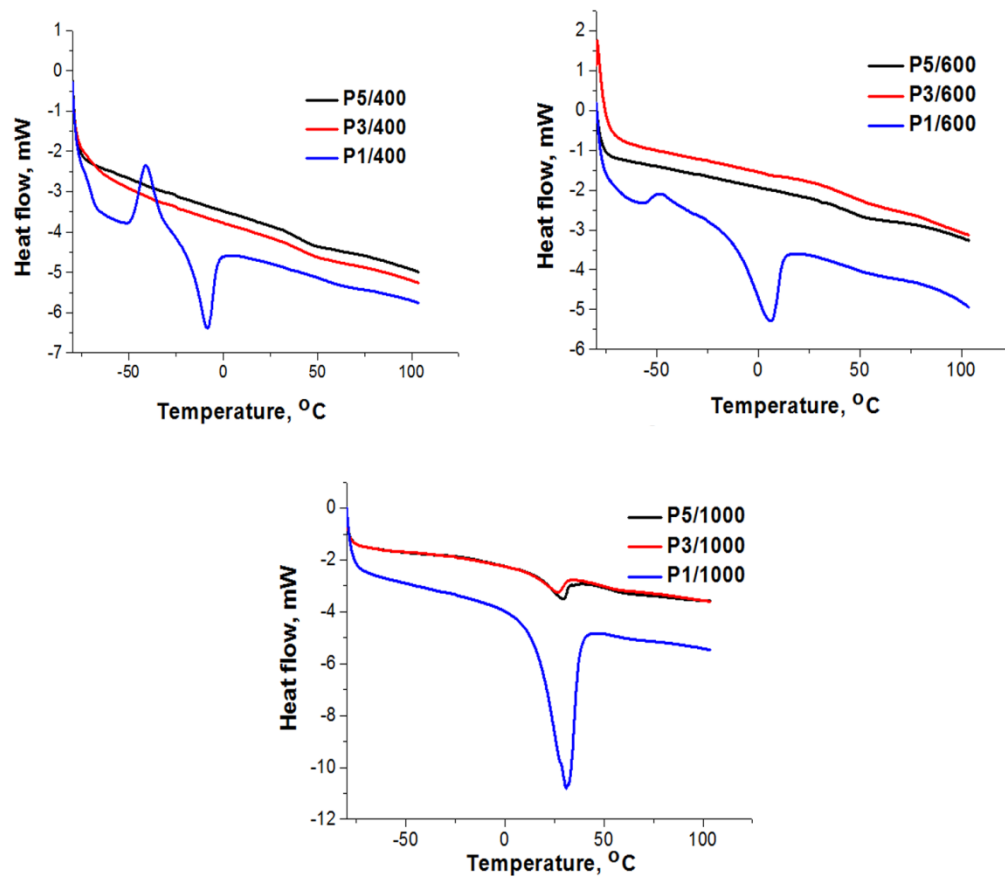
695 Figure 4  
696



697  
698  
699  
700  
701  
702  
703  
704  
705  
706  
707  
708  
709  
710  
711  
712  
713  
714  
715  
716  
717  
718

ACCEPTED

719 Figure 5  
720



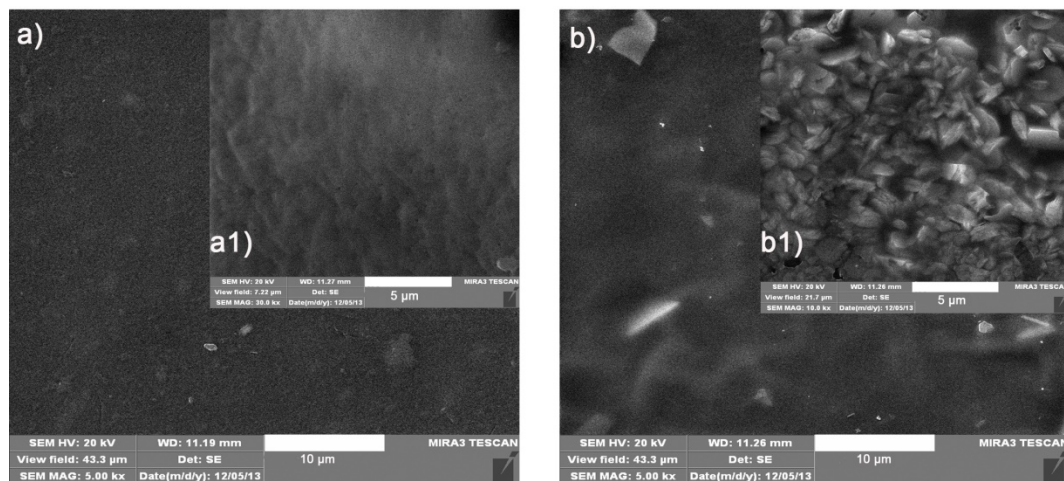
721  
722  
723  
724  
725  
726  
727  
728  
729  
730  
731  
732  
733  
734  
735  
736  
737  
738  
739  
740  
741  
742



743 Figure 6

744

745



746

747

748

749

750

